JOURNAL OF VIROLOGY, Oct. 2007, p. 11046–11053 Vol. 81, No. 20
0022-538X/07/$08.00+0 doi:10.1128/JVI.00388-07


# The Imidazopyrrolopyridine Analogue AG110 Is a Novel, Highly Selective Inhibitor of Pestiviruses That Targets the Viral RNA-Dependent RNA Polymerase at a Hot Spot for Inhibition of Viral Replication▽

Jan Paeshuyse,[1] Jean-Michel Chezal,[6] Matheus Froeyen,[1] Pieter Leyssen,[1] Hélène Dutartre,[3] Robert Vrancken,[2] Bruno Canard,[3] Carine Letellier,[2] Tong Li,[1] Harald Mittendorfer,[5] Frank Koenen,[2] Pierre Kerkhofs,[2] Erik De Clercq,[1] Piet Herdewijn,[1] Gerhard Puerstinger,[5] Alain Gueiffier,[4] Olivier Chavignon,[6] Jean-Claude Teulade,[6] and Johan Neyts[1]*

*Rega Institute for Medical Research, Katholieke Universiteit Leuven, Leuven, Belgium[1]; Veterinary and Agrochemical Research Centre, Ukkel, Belgium[2]; Laboratory AFMB-UMR 6098, Marseille, France[3]; Faculty of Pharmacy, EA 3857, University of Tours, Tours, France[4]; Department of Pharmaceutical Chemistry, Institute of Pharmacy, University of Innsbruck, Austria[5]; and Faculty of Pharmacy, University of Auvergne, Clermont-Ferrand, France[6]*

Received 23 February 2007/Accepted 26 July 2007

**Ethyl 2-methylimidazo[1,2-*a*]pyrrolo[2,3-*c*]pyridin-8-carboxylate (AG110) was identified as a potent inhibitor of pestivirus replication. The 50% effective concentration values for inhibition of bovine viral diarrhea virus (BVDV)-induced cytopathic effect, viral RNA synthesis, and production of infectious virus were 1.2 ± 0.5 μM, 5 ± 1 μM, and 2.3 ± 0.3 μM, respectively. AG110 proved inactive against the hepatitis C virus and a flavivirus. AG110 inhibits BVDV replication at a time point that coincides with the onset of intracellular viral RNA synthesis. Drug-resistant mutants carry the E291G mutation in the viral RNA-dependent RNA polymerase (RdRp). AG110-resistant virus is cross-resistant to the cyclic urea compound 1453 which also selects for the E291G drug resistance mutation. Moreover, BVDV that carries the F224S mutation (because of resistance to the imidazopyridine 5-[(4-bromophenyl)methyl]-2-phenyl-5*H*-imidazo[4,5-*c*]pyridine [BPIP]and VP32947) is also resistant to AG110. AG110 did not inhibit the in vitro activity of recombinant BVDV RdRp but inhibited the activity of BVDV replication complexes (RCs). Molecular modeling revealed that E291 is located in a small cavity near the tip of the finger domain of the RdRp about 7 Å away from F224. Docking of AG110 in the crystal structure of the BVDV RdRp revealed several potential contacts including with Y257. The E291G mutation might enable the free rotation of Y257, which might in turn destabilize the backbone of the loop formed by residues 223 to 226, rendering more mobility to F224 and, hence, reducing the affinity for BPIP and VP32947. It is concluded that a single drug-binding pocket exists within the finger domain region of the BVDV RdRp that consists of two separate but potentially overlapping binding sites rather than two distinct drug-binding pockets.**

The *Bovine viral diarrhea virus* (BVDV) is the prototype of the genus *Pestivirus* within the family of the *Flaviviridae*. The genus *Pestivirus* contains other important animal pathogens such as the classical swine fever virus (CSFV) and the border disease virus (BDV) that cause disease in pigs and sheep, respectively. Two biotypes of BVDV exist, a cytopathogenic (cp) and a noncytopathogenic (ncp) (22). In cattle BVDV causes a range of clinical manifestations varying from the subclinical to death (21). For the United States alone this translates roughly into a loss of $10 to $40 million per million calvings (15). Losses are projected in reduced milk production, reduced reproductive performance, growth retardation, and increased mortality among young stock (15). Also, the CSFV can be responsible for major economic losses, especially in countries with an industrialized pig production (10).

Regardless of the availability of vaccines against BVDV and CSFV and the implementation of elaborate eradication or control programs (14, 35), both viruses remain an agronomical burden. A novel approach to rapidly contain outbreaks of CSFV infections could be the prophylactic use, on farms located in close proximity to the infected farm, of antiviral agents that specifically inhibit the replication of the virus. Antiviral treatment might result in almost immediate protection against infection (protection following vaccination is only obtained 10 to 14 days later) and hence prevent transmission of the virus (and avoid large-scale culling of healthy animals). Other possible uses for antipestivirus drugs could be (i) treatment of valuable animals in zoologic collections, (ii) treatment of expensive animals in breeding programs and in vitro embryo production (36), or (iii) curing established cell lines from contaminating pestiviruses (9, 13).

Recently, we reported on the identification and mechanism of action of a potent inhibitor of pestivirus replication, i.e., 5-[(4-bromophenyl)methyl]-2-phenyl-5*H*-imidazo[4,5-*c*]pyridine (BPIP) (29). Interestingly, this compound was shown to be cross-resistant and to select for the same drug resistance

* Corresponding author. Mailing address: Rega Institute for Medical Research, Minderbroedersstraat 10, B-3000 Leuven, Belgium. Phone: 32 16 337341. Fax: 32 16 337340. E-mail: johan.neyts@rega.kuleuven.be.

▽ Published ahead of print on 8 August 2007.

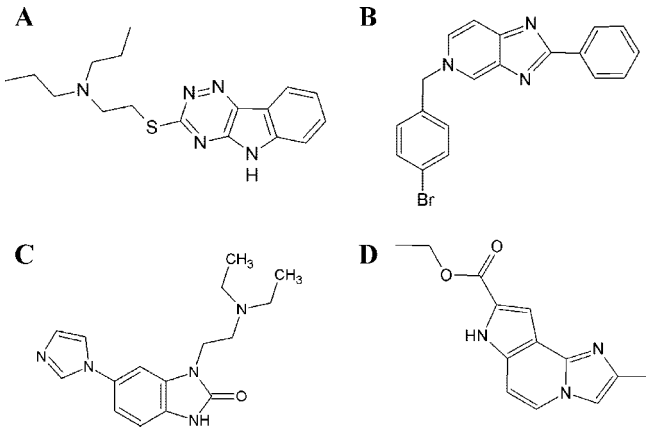


FIG. 1. Structural formulas of different antipestivirus compounds. (A) VP32947 (*N*-propyl-*N*-[2-(2*H*-1,2,4-triazino[5,6-*b*]indol-3-ylthio)ethyl]-1-propanamine) (1). (B) BPIP (5-[(4-bromophenyl)methyl]-2-phenyl-5*H*-imidazo[4,5-*c*]pyridine) (29, 30). (C) Compound 1453 [1-[2-(diethylamino) ethyl]-6-(1*H*-imidazol-1-yl)-1,3-dihydro-2*H*-benzimidazol-2-one] (37). (D) AG110 (ethyl 2-methylimidazo[1,2-*a*]pyrrolo[2,3-*c*]pyridin-8-carboxylate).

mutation (F224S) as an unrelated antipestivirus compound, *N*-propyl-*N*-[2-(2*H*-1,2,4-triazino[5,6-*b*]indol-3-ylthio)ethyl]-1-propanamine (VP32947) (1).

Here, we report on the activity and mechanism of action of an imidazopyrrolopyridine (AG110) as a novel inhibitor of the replication of pestiviruses. Surprisingly, AG110 (i) interacts with the viral polymerase at a position that is only 7 Å away from F224 and (ii) is cross-resistant with BPIP and VP32947. This region, F224 to E291, in the finger domain of the polymerase appears to be a hot spot for inhibition of viral replication.

## MATERIALS AND METHODS

**Compounds.** The synthesis of AG110 (ethyl 2-methylimidazo[1,2-*a*]pyrrolo[2,3-*c*]pyridin-8-carboxylate) will be reported elsewhere. BPIP (Fig. 1B) (29, 30), VP32947 (1), and the cyclic urea derivative compound 1453 (1-[2-(diethylamino)ethyl]-1,3-dihydro-6-(1*H*-imidazol-1-yl)-2*H*-benzimidazol-2-one) (Fig. 1C) (37) were synthesized by standard methods. 3′-dGTP and 2′-*C*-methylguanosine-5′-triphosphate (2′-*C*-Me-GTP) were purchased from Trilink (San Diego, CA).

**Solubility determination.** A serial dilution series of compound in either cell culture medium or 1× polymerase buffer (see below) was incubated for 1 h at 37°C on a rocking platform, after which the dilutions were centrifuged at 13,000 rpm for 5 min, and 100 μl of supernatant was transferred in a UV-STAR 96-well plate (Greiner Bio-one, Wemmel, Belgium). A standard curve was generated by making serial dilutions of the compound in 20% acetonitrile and 80% universal aqueous buffer (pH 7.4, 45 mM ethanolamine, 45 mM potassium dihydrogen phosphate, and 45 mM potassium acetate in water). Optical densities were determined at a wavelength of 300 nm.

**Cells and viruses.** Madin-Darby bovine kidney (MDBK) cells were grown in minimal essential medium (MEM) supplemented with 5% heat-inactivated fetal calf serum (FCS) (Integro, Zaandam, The Netherlands). FCS was shown to be free of BVDV type 1 (BVDV-1) and BVDV-2 by reverse transcription-PCR (RT-PCR) (19). Porcine kidney cells (PK15) were grown in MEM supplemented with 10% heat-inactivated FCS. First-passage BVDV strain NADL stock was generated from pNADLp15a as previously described (39). BPIP-resistant (BPIP$^r$) BVDV derived from a pNADLp15a plasmid containing the F224S mutation in the NS5B gene was generated as described previously (29). The CSFV strain Alfort was obtained from the Institut für Virologie, Hannover, Germany. BVDV-1 ncp Marloie and BVDV-2 ncp 3435 are field isolates obtained by the Veterinary and Agrochemical Research Center (Ukkel, Belgium). BDV ncp Aveyron was obtained from E. Thiry, University of Liège, Belgium. Human hepatoma cells (Huh 7) containing subgenomic hepatitis C virus (HCV) replicons $I_{389}$luc-ubi-neo/NS3-3′/5.1 (Huh 5-2) were kindly provided by R. Bartenschlager (University of Heidelberg, Germany) and were used to assess activity against HCV (23). Huh 5-2 cells were grown in Dulbecco's modified Eagle's medium (Gibco) supplemented with 10% heat-inactivated FCS (Integro), 1× nonessential amino acids (Gibco), 100 IU/ml penicillin (Gibco), 100 μg/ml streptomycin (Gibco), and 250 μg/ml geneticin (Gibco). Yellow fever virus (YFV) 17D was the vaccine strain Stamaril from Aventis Pasteur S. A.

**Antiviral assays.** Antiviral assays were performed as described previously (29). In brief, the appropriate cells were seeded at a density of $5 \times 10^3$ per well in 96-well cell culture plates. Following a 24-h incubation at 37°C and 5% $CO_2$, medium was removed, and threefold serial dilutions of the test compounds were added in a total volume of 100 μl, after which the cells were infected with the appropriate virus (except for Huh 5-2 replicon-containing cells). After 3 days medium was removed, and the following steps were carried out: (i) the cytopathic effect (CPE) induced by BVDV cp strains was quantified using the MTS/PMS]5-dimethylthiazol-2-yl)-5-(3-carboxymethoxy phenyl)-2-(4-sulfophenyl)-2*H*-tetrazolium salt and phenazine methosulfate] method (Promega, Leiden, The Netherlands); (ii) the number of foci was assessed by means of an immunohistochemical method for BVDV ncp strains, CSFV, and BDV; and (iii) the Steady-Glo luciferase assay system (Promega) was used to asses the effect on HCV replicon replication. The 50% effective concentration ($EC_{50}$) was defined as the concentration of compound that offered 50% protection of the cells against virus-induced CPE or a 50% reduction in foci or luciferase signal and was calculated using linear interpolation or, for the immunohistochemical assays, with the method of Reed and Muench (31).

Antiviral assays against a selection of DNA and RNA viruses were based on inhibition of virus-induced cytopathicity in either E6SM cells (herpes simplex virus type 1 [HSV-1], HSV-2, vaccinia virus, vesicular stomatitis virus), human embryonic lung cells (varicella-zoster virus and human cytomegalovirus), HeLa cells (respiratory syncytial virus), or Vero cells (YFV, coxsackie B4 virus, parainfluenza 3 virus, Sindbis virus, Punta Toro virus, reovirus type 1), according to previously established procedures (6–8, 28).

**Cytostatic assay.** MDBK or Huh 5-2 cells were seeded at a density of $5 \times 10^3$ cells per well of a 96-well plate in MEM-FCS; 24 h later, serial dilutions of the test compounds were added. Cells were allowed to proliferate for 3 days at 37°C, after which the cell number was determined by means of the MTS/PMS method (Promega). The percent cell growth was calculated as the ratio of the optical density at 490 nm ($OD_{490\ nm}$) of cells treated with a certain dilution of compound to the $OD_{490\ nm}$ of cells left untreated: ($OD_{treated}$/($OD_{control}$). The 50% cytostatic concentration ($CC_{50}$) was defined as the concentration that inhibited the proliferation of exponentially growing cells by 50% and was calculated using linear interpolation.

**Time-of-drug-addition studies.** MDBK cells ($3.5 \times 10^4$ cells/well) were seeded in 24-well culture plates. Cultures were inoculated with BVDV (strain NADL; multiplicity of infection of 2). The inoculum was removed following a 1-h incubation period, and cells were washed three times with prewarmed phosphate-buffered saline. To obtain precise information on the replication kinetics of BVDV in untreated cultures, supernatant and cells were harvested every 2 h, and samples were stored at −80°C until further use. In a parallel set of cultures, the test compounds (at 15 μM) were added at different time points after infection. Cultures were further incubated until 24 h postinfection, at which time cell culture supernatant was collected and stored at −80°C until further use.

**Virus yield assay.** MDBK cells were seeded at a density of $5 \times 10^3$ cells per well of a 96-well plate in MEM-FCS and were infected 24 h later with 10-fold serial dilutions of culture supernatant. After 4 days, the medium was removed, and cultures were fixed with 70% ethanol, stained with Giemsa solution, washed, and air dried. Virus-induced CPE was recorded microscopically, and the viral titer was quantified according to the method of Reed and Muench (31). Viral titers were expressed as the cell culture 50% infectious dose per ml.

**Isolation of AG110$^r$ BVDV.** AG110-resistant (AG110$^r$) virus was generated by culturing wild-type BVDV in MDBK cells in the presence of increasing concentrations of the compound in a 48-well plate. After 3 days of cultivation, cultures were subjected to freeze-thaw cycling. Lysates of infected and treated cultures that exhibited CPE under drug pressure were used to infect new cell monolayers. These were further incubated in the presence of increasing concentrations of the compound. The procedure was repeated (25 passages) until drug-resistant virus was selected.

**RNA isolation.** Viral RNA was isolated from cell culture supernatant using a QIAamp viral RNA minikit (QIAGEN, Venlo, The Netherlands). Total cellular RNA was isolated from cells using an RNeasy minikit (QIAGEN).

**RT-qPCR.** A 25-μl RT-quantitative PCR (RT-qPCR) reaction mixture contained 12.5 μl of 2× reaction buffer (Eurogentec, Seraing, Belgium), 6.3 μl of

TABLE 1. Effect of AG110 on the in vitro replication of various members of the family of the *Flaviviridae*

| Virus | Strain or genotype | Biotype | $EC_{50}$ (μM) of AG110 as determined by:[a] | | | | |
|---|---|---|---|---|---|---|---|
| | | | CPE assay | IHC assay | RNA yield | Virus yield | Luciferase assay |
| BVDV-1 | Marloie | ncp | | 5.9 ± 0.9 | | | |
| | NADL | cp | 1.2 ± 0.5 | 7 ± 1 | 5 ± 1 | 2.3 ± 0.3 | |
| BVDV-2 | 3435 | ncp | | 19 ± 0 | | | |
| CSFV | Alfort | | | 10 ± 6 | | | |
| BDV | Aveyron | | | 6 ± 1 | | | |
| HCV | 1b | | | | | | >50 |
| YFV | 17D | | >50 | | | | |

[a] The $EC_{50}$ for inhibition of viral replication was assessed by either a CPE reduction assay, an immunohistochemical (IHC) assay, an RNA or virus reduction assay, and a luciferase assay for the virus strains indicated. Data are mean values ± standard deviations for three or more independent experiments.

$H_2O$, 300 nmol/liter forward primer (5′-TGAGCTGTCTGAAATGGTCGA TT), 300 nmol/liter reverse primer (AGAAATACTGGGTCATCTGATGC AA), 300 nmol/liter TaqMan probe (6-FAM-CGAAGCAGGTTACCAAGGA GGCTGTTAGGA-TAMRA, where FAM is 6-carboxyfluorescein and TAMRA is 6-carboxytetramethylrhodamine), and 5 μl of total cellular or viral RNA extract. The RT step was performed at 48°C for 30 min and 15 min at 95°C with subsequent PCR amplification of 40 cycles of denaturation at 94°C for 20 s and annealing and extension at 60°C for 1 min in an ABI 7000 sequence detector.

**Sequencing.** PCR fragments that cover the entire nonstructural protein coding region of the BVDV genome were generated and analyzed using the cycle sequencing method (ABI Prism BigDye Terminator Cycle Sequencing Ready Reaction Kit). Both DNA strands were sequenced. Sequence data were obtained using an ABI 373 Automated Sequence Analyser (Applied Biosystems), and sequences were analyzed using the Vector NTI software package (Invitrogen, Merelbeke, Belgium). To assess the prevalence of the identified mutation(s) in the viral population, the region of the BVDV genome that harbors the mutation(s) was cloned in a pCR4-Topo vector and transformed into TOP10 chemically competent bacterial cells that were plated on selective LB agar plates containing 100 μg/ml ampicillin. Twenty colonies were picked and grown overnight in LB medium supplemented with 100 μg/ml ampicillin. Plasmids were isolated from these overnight cultures and sequenced using the M13 forward and reverse primers.

**RC assay.** The replication complex (RC) assay is essentially similar to the published procedure by Sun and colleagues (37). In brief, BVDV-infected MDBK cells were suspended in ice-cold hypotonic buffer A (10 mM Tris-HCl [pH 7.4], 1.5 mM $MgCl_2$) and were incubated for 30 min on ice, after which they were further disrupted by 20 strokes with a Dounce homogenizer. The disrupted cells were pelleted by centrifugation at 1,000 × *g* for 5 min at 4°C. The supernatant fraction, containing cytoplasmic material and plasma membranes, was concentrated by high-speed centrifugation at 200,000 × *g* for 30 min at 4°C. The pellet was resuspended in 120 μl of buffer B (10 mM Tris-HCl [pH 8.0], 10 mM NaCl, 15% glycerol) and used for an RNA polymerase assay. Replicase reactions were carried out in a total volume of 50 μl in 50 mM HEPES (pH 8.0), 50 mM potassium acetate, 3 mM $MgCl_2$, 10 mM dithiothreitol, 5 mM creatine phosphate, 25 μg/ml creatine phosphokinase, 1 mM ATP, 0.5 mM GTP, 0.5 mM CTP, 40 μM UTP, 10 μCi of [α-$^{33}$P]UTP (3,000 mCi/mmol) (Amersham, Uppsala, Sweden), 40 U of RNasin (Promega), and 10 μl of the membrane preparation. Following incubation at 30°C for 2 h, water was added to a volume of 100 μl, and the reactions were stopped by adding 350 μl of RLT buffer. Total RNA was extracted with an RNeasy kit (QIAGEN) according to the manufacturer's instruction. The RNA products were diluted with glyoxal sample loading dye (Ambion, Austin, TX) and analyzed on a 1% denaturing glyoxal-agarose gel. Next, agarose gels were dried, and the radioactivity incorporated into viral RNA was quantified using ImageQuant software for the Storm 820 PhosphorImager (Amersham).

**RdRp reaction.** BVDV (NADL) RNA-dependent RNA polymerase (RdRp) was expressed and purified as described before (41). The purified BVDV polymerase (100 nM) was mixed with 100 μM GTP (containing 8.3 μM [$^3$H]GTP; Amersham) and increasing concentrations of inhibitor (0,1 μM, 10 μM, 100 μM, or 500 μM) in 50 mM HEPES, pH 8.0, 10 mM KCl, 10 mM dithiothreitol, 1 mM $MgCl_2$, 2 mM $MnCl_2$, and 0.5% Igepal (Sigma). Enzyme mix and inhibitors were preincubated in order to favor an enzyme-inhibitor interaction before RNA binding in case of competition for the RNA binding site. Reactions were started by the addition of 100 nM poly(C) (about 500 nucleotides in size) template. Reactions mixtures were incubated at 30°C, and reactions were stopped by addition of 50 mM EDTA after 1, 5, or 15 min. Samples were transferred onto DE-81 filters, washed with 0.3 M ammonium formate solution, and dried. Radioactivity bound to the filter was determined by liquid scintillation counting.

**Molecular modeling.** The published X-ray structure of the BVDV RdRp (PDB entry 1S48) (5) was used in all docking experiments. Selenium atoms in the selenomethionine residues were modified back to sulfur atoms to get methionine residues. The inhibitor AG110 was drawn using the programs JChemPaint (17) and BUILD3D (34). The molecular geometry was fed into GAMESS for geometry optimization using the AM1 force field (33). Polar hydrogen atoms were added to the enzyme and inhibitor structures using the AutoDockTools package (32). AG110 was docked in the cavity in which E291 is located by means of the Autodock, version 3.05, software (27). The top 10 docked ligand conformations were examined, and finally the conformation with the top Autodock score was selected as being a good representative of these 10 docked conformations. Short (300 ps) molecular dynamics trajectories of the wild-type enzyme and E291G mutant were calculated using Amber software (3) following a standard protocol (20). The last 100 ps of these trajectories were used to calculate average enzyme structures. Interactions (H bonds and hydrophobic) were calculated using Ligplot and HB-Plus (25, 40).

## RESULTS

**Antiviral activity of AG110.** A diverse library of ≈7,000 small molecules—most of which had been synthesized as potential nonnucleoside reverse transcriptase inhibitors of human immunodeficiency virus—was screened against BVDV. A lead compound (AG32; ethyl 2-bromo-7*H*-imidazo[1,2-*a*]pyrrolo[3,2-*c*]pyridine-8-carboxylate) was identified that selectively inhibited in vitro BVDV replication. A limited number (12) of analogues were synthesized in an attempt to improve the antiviral activity. AG110 (Fig. 1D) was identified as the most selective inhibitor of BVDV (NADL) replication in a multicycle growth assay in MDBK cells. The $EC_{50}$, as assessed by monitoring CPE reduction by the MTS/PMS method, was 1.2 ± 0.5 μM (Table 1). The compound inhibited virus-induced CPE formation in a dose-dependent manner (Fig. 2A) and inhibited CPE formation by 100% at concentrations higher than 3.7 μM. To confirm the anti-BVDV activity of AG110, the effect of the compound on viral RNA synthesis (Fig. 2B) and on infectious viral yield was determined (Fig. 2C). Overall, the pattern of inhibition of viral RNA synthesis and infectious virus yield were very similar (Fig. 2A, B, and C). The $EC_{50}$ for inhibition of viral RNA production in culture supernatant was 5 ± 1 μM and 2.3 ± 0.3 μM for inhibition of infectious virus yield. AG110 also inhibited the replication of a BVDV-1 ncp strain but appeared somewhat less effective against a BVDV-2 ncp strain (Table 1). The compound inhibited the replication of CSFV (strain Alfort) and BDV (strain

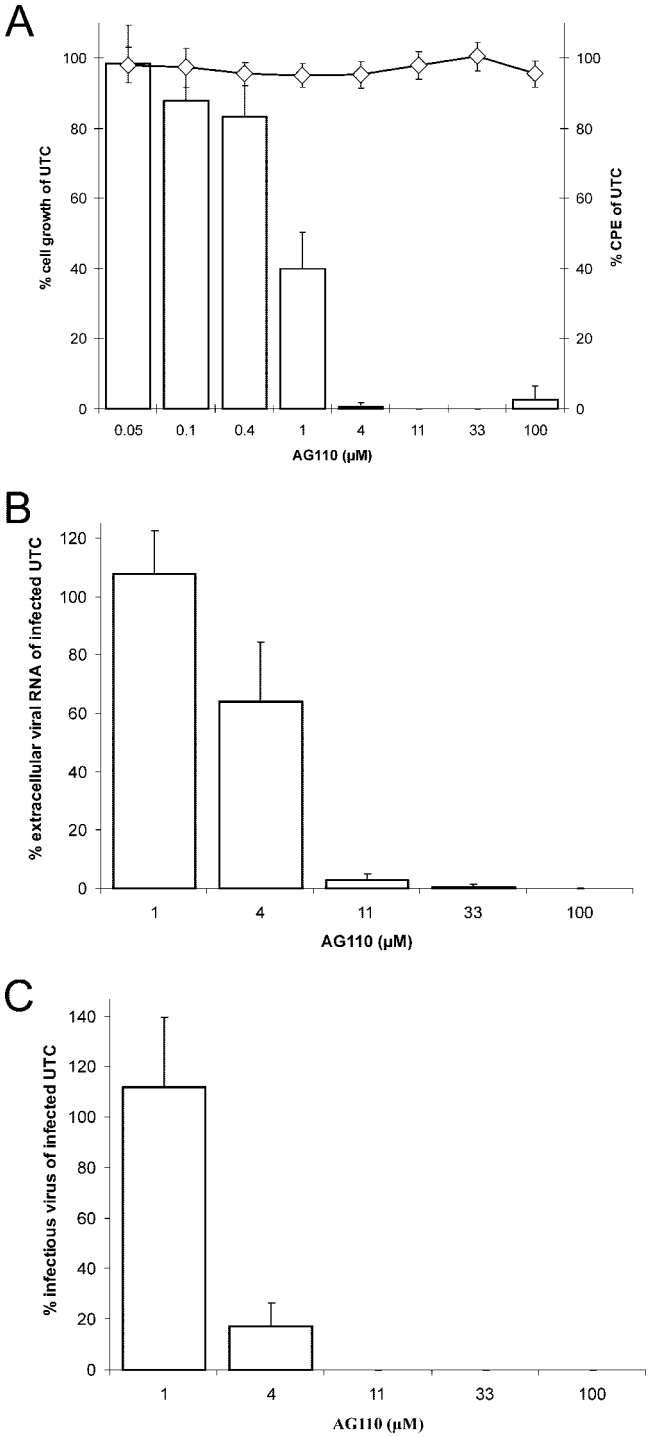


FIG. 2. (A) Effect of AG110 on BVDV (NADL)-induced CPE formation in MDBK cells (open bars) and on the proliferation of exponentially growing MDBK cells (open diamonds). (B) Inhibitory effect of AG110 on release of extracellular viral RNA. (C) Inhibitory effect of AG110 on infectious virus yield. Data are mean values ± standard deviations from three independent experiments. UTC, untreated control.

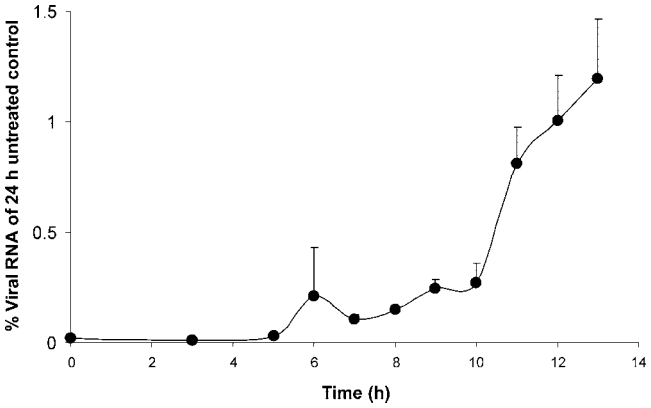


FIG. 3. Effect of time of drug addition on the antiviral activity of AG110. Intracellular viral RNA was monitored by RT-qPCR at 24 h postinfection in cells treated with AG110 (at a concentration of 20 μM and starting at different times postinfection) and compared with untreated infected cells. Values are expressed as percent viral RNA of untreated infected cells.

Aveyron) (Table 1). AG110 did not inhibit the replication of a selection of DNA viruses (HSV-1, HSV-2, vaccinia virus, and human cytomegalovirus) (data not shown) or a selection of RNA viruses (HCV [subgenomic replicon], YFV 17D, respiratory syncytial virus, vesicular stomatitis virus, coxsackie virus B4, Sindbis virus, reovirus type 1, and parainfluenza 3 virus) (data not shown).

AG110 had no inhibitory effect on the proliferation of exponentially growing uninfected host cells at concentrations up to 100 μM (Fig. 2A); the $CC_{50}$ was 212 ± 9 μM (data not shown). The solubility limit of AG110 was determined to be 500 μM in MEM and polymerase buffer (data not shown). Hence, a selectivity index (against BVDV NADL) or the ratio $CC_{50}/EC_{50}$ of about 180 was calculated.

**Time-of-drug-addition studies.** To understand at what time during the viral replication cycle AG110 interferes with viral replication, detailed time-of-drug-addition experiments were carried out. A single cycle of BVDV replication takes 13 h on average, and a gradual increase of intracellular viral RNA is noted at 6 to 8 h postinfection (29). This rise must coincide with the formation of functional RCs. A gradual loss in the antiviral efficacy of AG110 was noted when the compound was first added at a time point later than 6 h postinfection for intracellular RNA (Fig. 3).

**Isolation and characterization of drug-resistant viruses.** $AG110^r$ virus was selected by propagating BVDV (NADL) for 25 passages in the presence of increasing concentrations (1.1 to 30 μM) of the drug. The $AG110^r$ virus proved 40-fold less susceptible to the inhibitory effect of AG110 than the parent wild-type strain (Table 2) and about 20-fold less susceptible to BPIP (29) and VP32947 (1) and was not inhibited by compound 1453 (37). Interestingly, $BPIP^r$ virus, derived from a molecular clone that had the F224S reengineered in the NS5B gene, was fully resistant to inhibition by AG110 but retained wild-type sensitivity to compound 1453. In contrast, 2′-*C*-methylcytosine, a nucleoside analogue inhibitor of *Flaviviridae* (2, 11), was equipotent in inhibiting the replication of the wild-type virus and both resistant ($AG110^r$ or $BPIP^r$) viruses (Table 2). The $AG110^r$ virus carried a transition of T to C at position 11064, resulting in the E291G mutation in the RdRp.

**Effect on the BVDV RdRp and RCs.** AG110 and the nucleotide analogues 3′-dGTP and 2′-*C*-Me-GTP (that were included as positive controls) were studied for their effects on the

TABLE 2. Susceptibility of wild-type, AG110$^r$, and BPIP$^r$ BVDV to AG110, BPIP, VP32947, compound 1453, and 2′-*C*-methylcytosine

| Virus strain | $EC_{50}$ (μM) of the indicated inhibitor[a] | | | | |
|---|---|---|---|---|---|
| | AG110 | BPIP | VP32947 | 1453 | 2′-*C*-methylcytosine |
| Wild type (NADL) | 1.2 ± 0.5 | 0.21 ± 0.05 | 0.20 ± 0.05 | 58 | 1.4 ± 0.7 |
| AG110$^r$ BVDV | 53 ± 23 | 4.7 ± 0.8 | 3.4 ± 0.3 | >100 | 1.0 ± 0.3 |
| BPIP$^r$ BVDV | >100 | 57 ± 5 | >10 | 58 | 2.0 ± 0.1 |

[a] Data are mean values ± standard deviations for three independent experiments.

polymerase activity of highly purified BVDV RdRp. AG110 had no effect on the activity of the viral polymerase (Fig. 4). The 50% inhibitory concentration values for inhibition of BVDV polymerase activity were >200 μM for AG110, 2.4 μM for 2′-*C*-Me-GTP, and <1 μM for 3′-dGTP. Because AG110 had no inhibitory activity on the purified BVDV RdRp, the effect of the compound on viral RCs, isolated from MDBK cells that had been infected with the wild-type virus, was studied. AG110 inhibited the activity of the BVDV RCs in a dose-dependent manner (Fig. 5A and B). In contrast, AG110 had no inhibitory effect on the activity of RCs isolated from MDBK cells that had been infected with the laboratory-selected AG110$^r$ virus (Fig. 5A and B).

**Docking of AG110 in the BVDV RdRp crystal structure.** Molecular modeling revealed that E291 is located in a small cavity near the tip of the finger domain of the BVDV polymerase at a distance of only 7 Å from F224, the amino acid residue that is mutated in the case of resistance against BPIP or VP32947 (1, 29). Docking of AG110 in this cavity revealed possible interactions between the polymerase and AG110. The following possible interactions were calculated: (i) hydrophobic contacts of AG110 with L225, L244, I254, K255 and Y257; and (ii) a hydrogen bond between the naturally protonated N7 of AG110 and the side chain of E291 (Fig. 6A and B). Moreover, E291 can form other H bonds with surrounding residues (slightly different in the X-ray structure [Fig. 6B] and the averaged molecular dynamics structure [Fig. 6C]). There is also a hydrophobic stabilization between the side chains of E291 and E226. The E291G mutation will suppress the H-bond formation of residue 291 and hydrophobic interaction with E126. A void is created which facilitates a rotation of the Y257 side chain (Fig. 6C). This rotation might (i) change the shape of the cavity so that AG110 can no longer bind and (ii) destabilize the backbone of the loop formed by residues 220 to 230, rendering more mobility to the F224-containing loop and, hence, reducing the affinity for BPIP or VP32947.

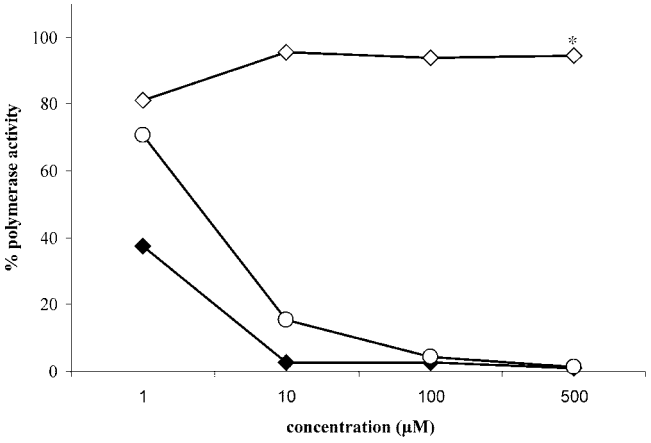


FIG. 4. Effect of AG110 (open diamonds), 2′-*C*-Me-GTP (open circles), and 3′-dGTP (filled diamonds) on the activity of purified BVDV RdRp using poly(C) as a template. Data are from a typical experiment and are expressed as the percentage of the untreated control. *, maximum concentration of AG110 tested was 200 μM.

## DISCUSSION

A small molecule, AG110, was identified (following limited lead optimization) as a selective in vitro inhibitor of the replication of pestiviruses. The compound proved active against both cp and ncp biotypes of BVDV-1, was somewhat less effective against BVDV-2, and also inhibited the replication of

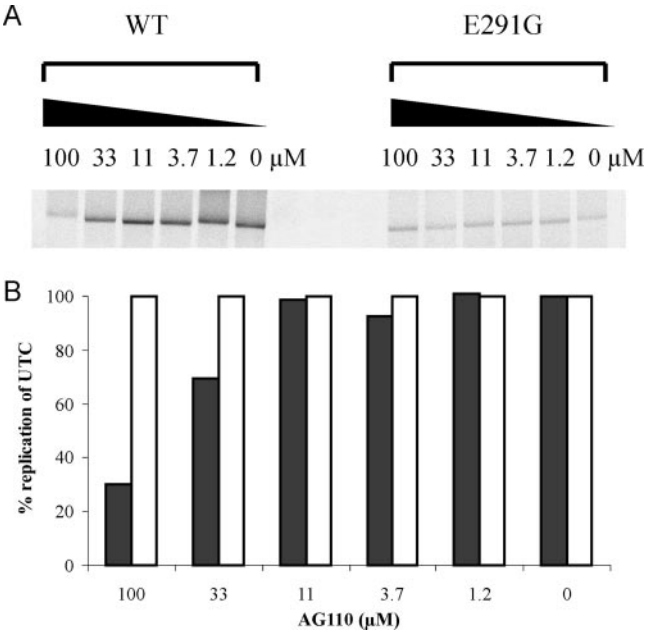


FIG. 5. Effect of AG110 on the activity of RCs isolated at 14 h postinfection from MDBK cells that had been infected with wild-type (NADL) or with the selected AG110$^r$ BVDV strain. (A) Reaction product of the RC assay was separated on a 1% agarose-glyoxal denaturing gel. RCs for this assay were either isolated from MDBK cells infected with wild-type virus or with the AG110$^r$ BVDV strain. (B) Densiometric analysis of the autoradiograph depicted in panel A. Black bars represent activity of wild-type (NADL) RCs, and open bars represent activity of RCs from cells infected with AG110$^r$ virus. UTC, untreated control; WT, wild type.

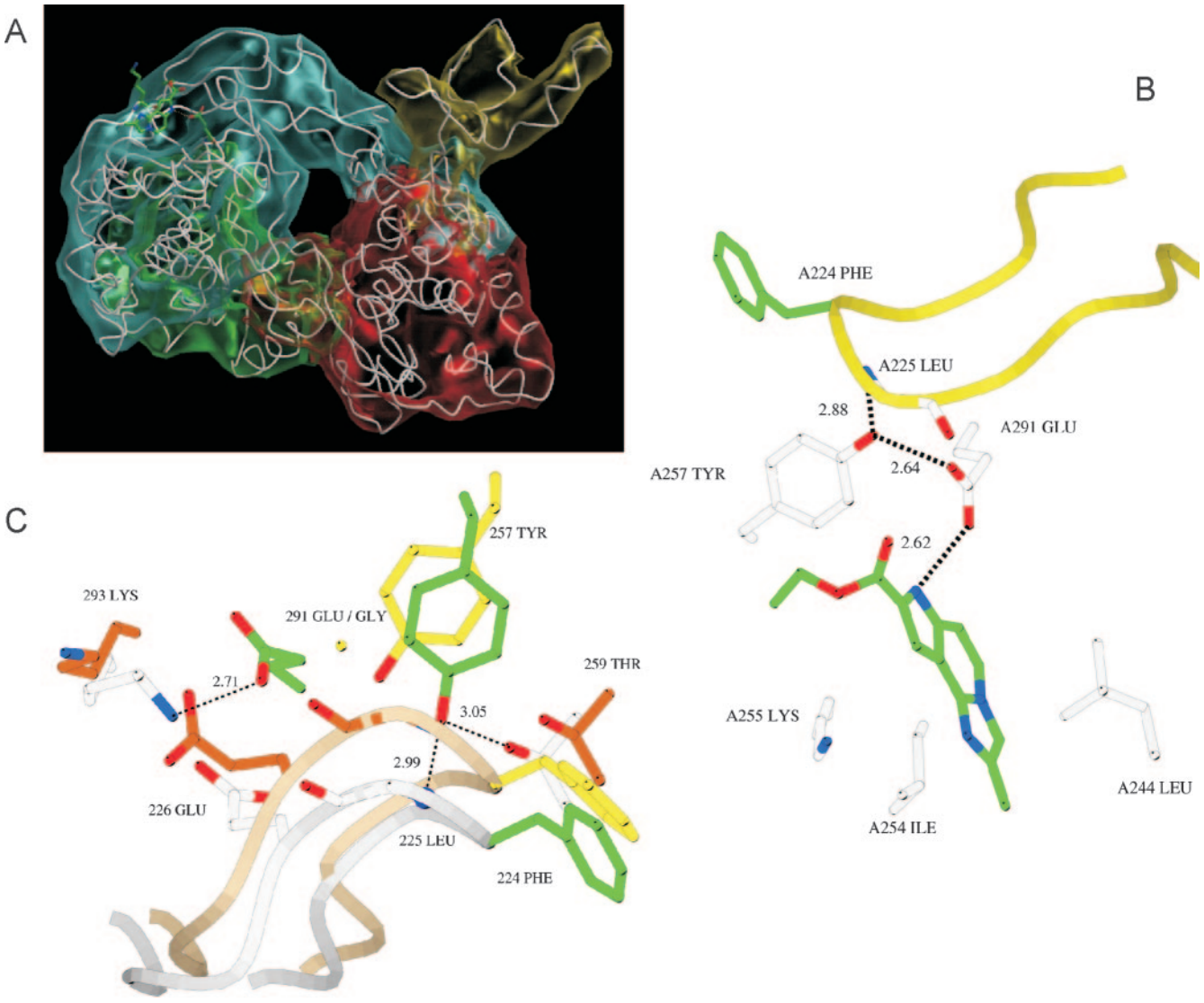


FIG. 6. Modeling of AG110 near the position of E291 in RdRp. (A) Overview of the entire structure of the RdRp of BVDV with AG110 docked in the vicinity of E291. The BVDV polymerase domains are shown in yellow (N-terminal domain, residues 1 to 138), blue (fingers, residues 139 to 313 and 351 to 410), green (palm, residues 314 to 350 and 411 to 500), or red (thumb, residues 501 to 679). (B) Detail of the pocket of the RdRp that presumably interacts with AG110. One predicted hydrogen bond between the naturally protonated N7 of AG110 and the side chain of E291 is shown. Residues involved in hydrophobic contact with AG110 are shown (white carbons). (C) Effect of the E291G mutation on the F224 residue. Superposition of average structures obtained by molecular dynamics of the wild-type and E291G mutant enzyme. The loop formed by residues 210 to 230 is drawn as a gray (wild type) or brown (E291G) ribbon. Carbon atoms in the wild-type enzyme are green or white; those in the mutant are yellow and dark brown. The removal of the E291 side chain has a dramatic effect on its surroundings. The creation of a void makes residue 257 swing to the left, breaking all interactions with the backbone atoms of the loop. The hydrophobic interaction between the asparagine residues 291 and 226 is also lost by the mutation. These changes might influence the orientation and position of F224. Picture generated using Bobscript, Molscript and Raster 3D (12, 16, 26).

CSFV and BDV. The compound proved inactive against the HCV and against the flavivirus YFV (vaccine strain 17D).

The time point at which AG110 exerts its activity coincides with the onset of viral RNA synthesis (i.e., at about 6 h postinfection). The addition of the compound at a time point before onset of intracellular viral RNA synthesis resulted in complete inhibition of viral RNA production, whereas the addition of AG110 at later time points resulted in a gradual loss of antiviral activity. These data suggest that AG110 interferes with the formation or functioning of the RC of the virus. In vitro selected AG110$^r$ BVDV carries an E291G mutation in the polymerase gene. Compound 1453, a cyclic urea with (modest) antipestivirus activity (37) proved to be cross-resistant with AG110. This can be explained by the observation that the compound 1453-resistant virus (akin to AG110$^r$ virus) also carries the E291G mutation. BPIP$^r$ and VP32947-resistant (VP32947$^r$) viruses were shown earlier to carry the F224S mutation (29). The BPIP$^r$ and VP32947$^r$ viruses were surprisingly also no longer susceptible to inhibition by AG110 (Table 2). This may be explained by the proximity (7 Å) of E291 and

F224 in the RdRp structure. The F224S mutation (selected by antiviral pressure with either BPIP or VP32947) might influence the structure of the RdRp in the close vicinity of residue 224. This might result in a change in the structure of the region where AG110 and compound 1453 bind. The fact that compound 1453 does inhibit BPIP$^r$ virus whereas AG110 does not might possibly be explained by particular differences in the binding of AG110 and compound 1453 in the pocket around E291. Indeed, docking of compound 1453 in the pocket reveals no hydrogen bonds, whereas AG110 is believed to interact with the same pocket through a hydrogen bond. The fact that AG110$^r$ virus is about 20-fold less susceptible to inhibition by BPIP and VP32947 may be explained by the potential of the E291G mutation to abolish the interaction between E291 and Y257, enabling the rotation of Y257 and thus destabilizing the backbone loop formed by residues 223 to 226. This instability might result in an increased mobility of F224 and, hence, a reduced affinity for BPIP and VP32947.

Although the genotyping and cross-resistance studies provide strong evidence for interference with the viral polymerase activity, AG110 had no effect on the activity of the highly purified RdRp. The viral polymerase assay was validated by demonstrating that 2′-*C*-Me-GTP and a related molecule inhibited the BVDV RdRp activity. Similarly, (i) the cyclic urea derivative compound 1453 (37), (ii) VP32947 (1), and (iii) BPIP (29) also had limited, if any, inhibitory effect on the highly purified RdRp. Within the cell, BVDV NS5B functions in the context of membrane-bound RCs that consist of several virus-encoded proteins, host proteins, and various forms of viral RNA (37, 38). We therefore evaluated the effect of AG110 on RCs isolated from MDBK cells that had been infected with either the wild-type virus or the AG110$^r$ virus. AG110 inhibited the functioning of the wild-type RC but not that of the mutant. Although AG110 inhibited wild-type RCs, it did so less efficiently than it inhibited viral replication. Similar observations were made for several nonnucleoside inhibitors of HCV RC (24). This may be explained by (i) a specific conformation of the viral polymerase in the replicase complex because of productive interaction with template RNA, (ii) protein-protein interaction between NS5B and other viral nonstructural proteins or host proteins occluding compound binding sites on NS5B, and (iii) oligomerization of NS5B during formation of the RC (24). One possible explanation for the fact that AG110 does inhibit the function of the RC but not of the purified polymerase may be that the compound, following its interaction with NS5B, disturbs the formation/stability/function of the RC.

The crystal structure of the RdRp of BVDV (5) reveals that E291G is located in a small cavity near the base of the loops of the finger domain that encloses the active site of the RdRp. Residue E291 (in boldface) is part of the highly conserved NC motif KRPRVIQYP**E**AKTR (18). A more complete (residues 78 to 679) crystal structure of the BVDV RdRp containing its amino-terminal domain was recently reported (4). Although the exact function of the N-terminal domain is not yet known, it was suggested (i) to be involved in both elongative and de novo RNA synthesis, (ii) to facilitate the translocation of the template in conjunction with the fingers, (iii) to recruit other polymerases into the RC, or (iv) to stabilize the fingertips during movement thereof (4). Interestingly, this crystal structure revealed hydrophobic interactions between the F224 residue and the N-terminal domain (4). Thus, binding of inhibitors, such as BPIP (29) or VP32947 (1) and likely also AG110 and compound 1453 (37), might disrupt these interactions and interfere with the function of the N-terminal domain. Possible binding of AG110 (or the other inhibitors) to the polymerase could result in reduced finger flexibility or impairment of the ability of the polymerase to translocate its template/product during polymerization. However, this hypothesis is somewhat contradicted by the lack of activity of AG110 in the in vitro recombinant RdRp assay. Also the generation of cocrystals of the BVDV RdRp with VP32947 (1) was not successful, and it was hypothesized that this was hampered by a dimer interface near the putative binding site of VP32947 (1) (in the vicinity of F224). It was suggested (i) that such a dimer could play an important role in the functioning of the replication complex and (ii) that the top of the finger domain may be a protein-binding site important for interaction with other proteins of the RC.

In conclusion, we here report on AG110, a novel, selective inhibitor of the replication of pestiviruses. The compound is cross-resistant with three other inhibitors of pestivirus replication, i.e., compound 1453 (37), BPIP (29), and VP32947 (1). These compounds select for mutations (amino acid E291 for AG110 and compound 1453 [37] or amino acid F224 for BPIP [29] and VP32947 [1]) within a region of the finger domain of the RdRp that is only 7 Å across. Obviously, the region of the polymerase in which these mutations are located (i) is crucial for the functioning of the polymerase and the viral RC and (ii) is apparently a hot spot binding site for selective inhibitors of pestivirus replication.

## ACKNOWLEDGMENTS

We thank Katrien Geerts and Geoffrey Férir for excellent technical assistance and Dominique Brabants, Chantal Biernaux, and Christiane Callebaut for dedicated editorial help.

This work was supported by a postdoctoral position of the Onderzoeksfonds of the Katholieke Universiteit Leuven to J.P. and by the VIZIER integrated project (LSHG-CT-2004-511960) from the European Union 6th PCRDT and Geconcerteerde Onderzoeksactie-Vlaanderen (GOA-2005/19, J.P.).

## REFERENCES

1. **Baginski, S. G., D. C. Pevear, M. Seipel, S. C. Sun, C. A. Benetatos, S. K. Chunduru, C. M. Rice, and M. S. Collett.** 2000. Mechanism of action of a pestivirus antiviral compound. Proc. Natl. Acad. Sci. USA **97:**7981–7986.
2. **Carroll, S. S., J. E. Tomassini, M. Bosserman, K. Getty, M. W. Stahlhut, A. B. Eldrup, B. Bhat, D. Hall, A. L. Simcoe, R. LaFemina, C. A. Rutkowski, B. Wolanski, Z. Yang, G. Migliaccio, R. De Francesco, L. C. Kuo, M. MacCoss, and D. B. Olsen.** 2003. Inhibition of hepatitis C virus RNA replication by 2′-modified nucleoside analogs. J. Biol. Chem. **278:**11979–11984.
3. **Case, D., T. E. Cheatham, T. Darden, H. Gohlke, R. Luo, K. M. Merz, A. Onufriev, C. Simmerling, B. Wang, and R. Woods.** 2007. The Amber biomolecular simulation programs. J. Comput. Chem. **26:**1668–1688.
4. **Choi, K. H., A. Gallei, P. Becher, and M. G. Rossmann.** 2006. The structure of bovine viral diarrhea virus RNA-dependent RNA polymerase and its amino-terminal domain. Structure **14:**1107–1113.
5. **Choi, K. H., J. M. Groarke, D. C. Young, R. J. Kuhn, J. L. Smith, D. C. Pevear, and M. G. Rossmann.** 2004. The structure of the RNA-dependent RNA polymerase from bovine viral diarrhea virus establishes the role of GTP in de novo initiation. Proc. Natl. Acad. Sci. USA **101:**4425–4430.
6. **De Clercq, E.** 1985. Antiviral and antimetabolic activities of neplanocins. Antimicrob. Agents Chemother. **28:**84–89.
7. **De Clercq, E., J. Descamps, G. Verhelst, R. T. Walker, A. S. Jones, P. F. Torrence, and D. Shugar.** 1980. Comparative efficacy of antiherpes drugs against different strains of herpes simplex virus. J. Infect. Dis. **141:**563–574.
8. **De Clercq, E., A. Holy, I. Rosenberg, T. Sakuma, J. Balzarini, and P. C. Maudgal.** 1986. A novel selective broad-spectrum anti-DNA virus agent. Nature **323:**464–467.

9. **Durantel, D., S. Carrouee-Durantel, N. Branza-Nichita, R. A. Dwek, and N. Zitzmann.** 2004. Effects of interferon, ribavirin, and iminosugar derivatives on cells persistently infected with noncytopathic bovine viral diarrhea virus. Antimicrob. Agents Chemother. **48:**497–504.
10. **Edwards, S., A. Fukusho, P. C. Lefevre, A. Lipowski, Z. Pejsak, P. Roehe, and J. Westergaard.** 2000. Classical swine fever: the global situation. Vet. Microbiol. **73:**103–119.
11. **Eldrup, A. B., C. R. Allerson, C. F. Bennett, S. Bera, B. Bhat, N. Bhat, M. R. Bosserman, J. Brooks, C. Burlein, S. S. Carroll, P. D. Cook, K. L. Getty, M. MacCoss, D. R. McMasters, D. B. Olsen, T. P. Prakash, M. Prhavc, Q. Song, J. E. Tomassini, and J. Xia.** 2004. Structure-activity relationship of purine ribonucleosides for inhibition of hepatitis C virus RNA-dependent RNA polymerase. J. Med. Chem. **47:**2283–2295.
12. **Esnouf, R. M.** 1999. Further additions to MolScript version 1.4, including reading and contouring of electron-density maps. Acta Crystallogr. **55:**938–940.
13. **Givens, M. D., D. A. Stringfellow, C. C. Dykstra, K. P. Riddell, P. K. Galik, E. Sullivan, J. Robl, P. Kasinathan, A. Kumar, and D. W. Boykin.** 2004. Prevention and elimination of bovine viral diarrhea virus infections in fetal fibroblast cells. Antivir. Res. **64:**113–118.
14. **Greiser-Wilke, I., B. Grummer, and V. Moennig.** 2003. Bovine viral diarrhoea eradication and control programmes in Europe. Biologicals **31:**113–118.
15. **Houe, H.** 2003. Economic impact of BVDV infection in dairies. Biologicals **31:**137–143.
16. **Kraulis, P. J.** 1991. MOLSCRIPT: a program to produce both detailed and schematic plots of protein structures. J. Appl. Crystallogr. **24:**946–950.
17. **Krause, S., E. L. Willighagen, and C. Steinbeck.** 2000. JChemPaint—using the collaborative forces of the Internet to develop a free editor for 2D chemical structures. Molecules **5:**93–98.
18. **Lai, V. C., C. C. Kao, E. Ferrari, J. Park, A. S. Uss, J. Wright-Minogue, Z. Hong, and J. Y. Lau.** 1999. Mutational analysis of bovine viral diarrhea virus RNA-dependent RNA polymerase. J. Virol. **73:**10129–10136.
19. **Letellier, C., P. Kerkhofs, G. Wellemans, and E. Vanopdenbosch.** 1999. Detection and genotyping of bovine diarrhea virus by reverse transcription-polymerase chain amplification of the 5′ untranslated region. Vet. Microbiol. **64:**155–167.
20. **Li, T., M. Froeyen, and P. Herdewijn.** 3 May 2007, posting date. Computational alanine scanning and free energy decomposition for E. coli type I signal peptidase with lipopeptide inhibitor complex. J. Mol. Graph. Model. doi:10.1016/j.mgm.2007.04.007.
21. **Lindberg, A. L.** 2003. Bovine viral diarrhoea virus infections and its control. A review. Vet. Q. **25:**1–16.
22. **Lindenbach, B. D., and C. M. Rice.** 2001. *Flaviviridae*: the viruses and their replication, p. 991–1041. *In* D. M. Knipe, P. M. Howley, D. E. Griffin, R. A. Lamb, M. A. Martin, B. Roizman, and S. E. Straus (ed.), Fields virology, 4th ed. Lippincott Williams and Wilkins, Philadelphia, PA.
23. **Lohmann, V., F. Korner, J. Koch, U. Herian, L. Theilmann, and R. Bartenschlager.** 1999. Replication of subgenomic hepatitis C virus RNAs in a hepatoma cell line. Science **285:**110–113.
24. **Ma, H., V. Leveque, A. De Witte, W. Li, T. Hendricks, S. M. Clausen, N. Cammack, and K. Klumpp.** 2005. Inhibition of native hepatitis C virus replicase by nucleotide and non-nucleoside inhibitors. Virology **332:**8–15.
25. **McDonald, I. K., and J. M. Thornton.** 1994. Satisfying hydrogen bonding potential in proteins. J. Mol. Biol. **238:**777–793.
26. **Merritt, E. A., and D. J. Bacon.** 1997. Raster 3D: photorealistic molecular graphics. Methods Enzymol. **277:**505–524.
27. **Morris, G. M., D. S. Goodsell, R. S. Halliday, R. Huey, W. E. Hart, R. K. Belew, and A. J. Olson.** 1998. Automated docking using a Lamarckian genetic algorithm and empirical binding free energy function. J. Comput. Chem. **19:**1639–1662.
28. **Neyts, J., A. Meerbach, P. McKenna, and E. De Clercq.** 1996. Use of the yellow fever virus vaccine strain 17D for the study of strategies for the treatment of yellow fever virus infections. Antivir. Res. **30:**125–132.
29. **Paeshuyse, J., P. Leyssen, E. Mabery, N. Boddeker, R. Vrancken, M. Froeyen, I. H. Ansari, H. Dutartre, J. Rozenski, L. H. Gil, C. Letellier, R. Lanford, B. Canard, F. Koenen, P. Kerkhofs, R. O. Donis, P. Herdewijn, J. Watson, E. De Clercq, G. Puerstinger, and J. Neyts.** 2006. A novel, highly selective inhibitor of pestivirus replication that targets the viral RNA-dependent RNA polymerase. J. Virol. **80:**149–160.
30. **Puerstinger, G., J. Paeshuyse, P. Herdewijn, J. Rozenski, E. De Clercq, and J. Neyts.** 2006. Substituted 5-benzyl-2-phenyl-5*H*-imidazo[4,5-*c*]pyridines: a new class of pestivirus inhibitors. Bioorg. Med. Chem. Lett. **16:**5345–5349.
31. **Reed, L. J., and A. H. Muench.** 1938. A simple method of estimating fifty percent endpoints. Am. J. Hyg. **27:**493–497.
32. **Rogers, J. P., A. E. Beuscher, M. Flajolet, T. McAvoy, A. C. Nairn, A. J. Olson, and P. Greengard.** 2006. Discovery of protein phosphatase 2C inhibitors by virtual screening. J. Med. Chem. **49:**1658–1667.
33. **Schmidt, M. W., K. K. Baldridge, J. A. Boatz, S. T. Elbert, M. S. Gordon, J. H. Jensen, S. Koseki, N. Matsunaga, K. A. Nguyen, S. Su, T. L. Windus, M. Dupuis, and J. A. Montgomery.** 1993. General atomic and molecular electronic structure system. J. Comput. Chem. **14:**1347–1363.
34. **Smith, D. H., N. A. B. Gray, J. G. Norse, and C. W. Crandell.** 1981. The Dendral project: recent advances in computer-assisted structure elucidation. Anal. Chim. Acta **133:**471–497.
35. **Stegeman, A., A. Elbers, H. de Smit, H. Moser, J. Smak, and F. Pluimers.** 2000. The 1997–1998 epidemic of classical swine fever in The Netherlands. Vet. Microbiol. **73:**183–196.
36. **Stringfellow, D. A., K. P. Riddell, M. D. Givens, P. K. Galik, E. Sullivan, C. C. Dykstra, J. Robl, and P. Kasinathan.** 2005. Bovine viral diarrhea virus (BVDV) in cell lines used for somatic cell cloning. Theriogenology **63:**1004–1013.
37. **Sun, J.-H., J. A. Lemm, D. R. O'Boyle II, J. Racela, R. Colonno, and M. Gao.** 2003. Specific inhibition of bovine viral diarrhea virus replicase. J. Virol. **77:**6753–6760.
38. **Uchil, P. D., and V. Satchidanandam.** 2003. Architecture of the flaviviral replication complex. Protease, nuclease, and detergents reveal encasement within double-layered membrane compartments. J. Biol. Chem. **278:**24388–24398.
39. **Vassilev, V. B., and R. O. Donis.** 2000. Bovine viral diarrhea virus induced apoptosis correlates with increased intracellular viral RNA accumulation. Virus Res. **69:**95–107.
40. **Wallace, A. C., R. A. Laskowski, and J. M. Thornton.** 1995. LIGPLOT: a program to generate schematic diagrams of protein-ligand interactions. Protein Eng. **8:**127–134.
41. **Zhong, W., L. L. Gutshall, and A. M. Del-Vecchio.** 1998. Identification and characterization of an RNA-dependent RNA polymerase activity within the nonstructural protein 5B region of bovine viral diarrhea virus. J. Virol. **72:**9365–9369.